VILNIUS UNIVERSITY

VYTAUTAS JAKŠTYS

APPLICATION OF CONTOUR DETECTION METHODS TO LATERAL CHROMATIC ABERRATION REDUCTION IN EYE FUNDUS IMAGES AND ROAD SURFACE DEFECT DETECTION

Summary of Doctoral Dissertation

Technological Sciences, Informatics Engineering (07 T)

VILNIUS, 2018

Doctoral thesis was written in 2013–2017 at the Vilnius University Institute of Data Science and Digital Technologies.

Scientific Supervisor

Dr. Virginijus Marcinkevičius (Vilnius University, Technological Sciences, Informatics Engineering – 07 T).

The defense council:

Chairman

prof. dr. Julius Žilinskas (Vilnius University, Technological Sciences, Informatics Engineering – 07 T).

Members:

prof. dr. Rimantas Vaicekauskas (Vilnius University, Technological Sciences, Informatics Engineering – 07 T),
prof. dr. Romualdas Baušys (Vilnius Gediminas Technical University, Technological Sciences, Informatics Engineering – 07 T),
prof. dr. Tomas Krilavičius (Vytautas Magnus University, Technological Sciences, Informatics Engineering – 07 T),
prof. dr. Audris Mockus (University of Tennessee, USA, Technological Sciences, Informatics Engineering – 07 T).

The thesis will be defended at the public session of the defense Council in the auditorium number 203 at Vilnius University at 09:30 on the 11th of June 2018.
The summary of the doctoral thesis was distributed on the 10th of May 2018.
A copy of the doctoral thesis is available for review at the Library of Vilnius University.

VILNIAUS UNIVERSITETAS

VYTAUTAS JAKŠTYS

KONTŪRO ATPAŽINIMO METODŲ TAIKYMAS SKERSINEI CHROMATINEI ABERACIJAI ŠALINTI AKIES DUGNO VAIZDUOSE IR KELIO DANGOS DEFEKTAMS ATPAŽINTI

Daktaro disertacijos santrauka

Technologijos mokslai, informatikos inžinerija (07 T)

VILNIUS, 2018

Disertacija rengta 2013–2017 metais Vilniaus universiteto Duomenų mokslo ir skaitmeninių technologijų institute.

Mokslinis vadovas – dr. Virginijus Marcinkevičius (Vilniaus universitetas, technologijos mokslai, informatikos inžinerija – 07 T).

Disertacija ginama viešame disertacijos Gynimo tarybos posėdyje:

Pirmininkas – prof. dr. Julius Žilinskas (Vilniaus universitetas, technologijos mokslai, informatikos inžinerija – 07 T).

Nariai:

prof. dr. Rimantas Vaicekauskas (Vilniaus universitetas, technologijos mokslai, informatikos inžinerija – 07 T),
prof. dr. Romualdas Baušys (Vilniaus Gedimino technikos universitetas, technologijos mokslai, informatikos inžinerija – 07 T),
prof. dr. Tomas Krilavičius (Vytauto Didžiojo universitetas, technologijos mokslai, informatikos inžinerija – 07 T),
prof. dr. Audris Mockus (Tenesio universitetas, JAV, technologijos mokslai, informatikos inžinerija – 07 T).

Disertacija bus ginama viešame disertacijos Gynimo tarybos posėdyje 2018 m. birželio 11 d. 09:30. Vilniaus universitete 203 auditorijoje.
Adresas: Akademijos g. 4, LT-08663 Vilnius, Lietuva.
Disertacijos santrauka išsiuntinėta 2018 m. gegužės 10 d.
Su disertacija galima susipažinti Vilniaus universiteto bibliotekoje ir VU interneto svetainėje adresu: *www.vu.lt/lt/naujienos/ivykiu-kalendorius*

1 Introduction

1.1 Research area

The results obtained in the dissertation relate to two areas of research: Image Analysis and Image Processing. The amount of visual information and data has grown so rapidly in various fields that there is a high need for processing to obtain meaningful information such as the recognition of an object, an object's contour, segmenting objects, etc. This area is called the Image Analysis Area. There are many different methods for the analysis of digital images and the recognition of objects and contours, but their accuracy is affected by images with a large color variance, non-uniform texture and different contour shapes. Such objects are road surface defects or timber knots, as shown on the left side of figure 1. There is an active contouring method for recognizing such objects. However, this method also was unable to accurately identify these contours, thus this research presents a new method for the identification of contours of road surface defects and timber knots. In the thesis, this new method was compared with other analyzed contour recognition methods.
The main purpose of the image processing area is to analyze and improve the image quality in order to make it as comfortable and as quick as possible for a person to understand or analyze it. Most of the different devices have image capture device, so it became important to improve them so the best quality images can be captured. As all cameras use lenses, one of the main obstacles is the appearance of chromatic aberration (ChA). Mechanically, this effect can be reduced by using achromatic, apochromatic, or diffractive lenses. However, when limiting the size of the camera, a mechanical solution is not suitable, as it takes up too much space inside the device, its weight and increased costs. For these reasons, there is a need for each optical system to have software that programmatically reduces or completely eliminates chromatic aberration. In this research, a wide range of methods were analyzed, chromatic aberration reduction methods were tested, and a new method for the reduction of lateral chromatic aberrations in the eye fundus images is presented using blood vessels' recognition, which can be applied to all eye fundus images without a camera.

1.2 Relevance of the problem

A widespread use of visual information has increased the demand not only for image quality enhancement but also for digital image analysis, object recognition, contour identification, etc. Digital image processing is relevant in many fields: astronomy (e.g. electromagnetic radiation), meteorology (e.g. weather forecasting), health service (e.g. positron emission tomography, magnetic resonance imaging, computed tomography, ultrasound, X-rays), archeology (e.g. image enhancement and recovery is used to restore fading images), forensics, warfare, manufacturing, engineering, etc. The experience gained by a person while growing up makes it easy for him to recognize the various objects and their contours. However, computer perception is a complicated action. The best methods detect objects and their contours in images with a low color variance and images with a lot of uniform texture. But in reality, such images are rare, so the accuracy of the

existing methods is greatly reduced when there is a high color variance in the image, the objects do not have a uniform texture, or their shape changes. Images in this group include timber knots, defect parts of the walls of buildings and road surface defects. At present, road work engineers measure road imperfections and decide on further road repairs, furniture makers recognize timber knots on the board and cover them with plaster, therefore, there is a need to create a method that would be able to accurately identify these contours.

A camera is being used to save visual information, which is constantly improved in order to produce a higher accuracy. But since all cameras use lenses, they inevitably face a variety of aberrations. The aberration distortion was tried to be reduced mechanically by using various achromatic, apochromatic or diffractive lenses. Since these lenses occupy extra space and are expensive to produce, they are not useful in the case of small cameras, such as portable eye fundus cameras. Therefore, various programmatic image correction methods for digital images are being developed to reduce the effect of chromatic aberration. In the literature, the methods that were able to reduce the effect of chromatic aberration usually required the camera with which the image was captured. Since blood vessels are visible in all eye fundus images, the recognized contours of blood vessels makes it possible to create a method that does not require the camera with which the image was captured.

1.3 Research objectives

The research objectives of this thesis are object contour detection and lateral chromatic aberration reduction when applying contour detection in digital images.

1.4 The aim and tasks of the research

Research aim:

1. To create a method for the reduction of the lateral chromatic aberration effect in eye fundus images as well as a method for road surface defect contour detection

To accomplish the aim of this research, the following tasks were performed:

1. Analysis of existing methods for contour recognition of objects that do not have a uniform texture and display a large color variance, and the creation of a method for contour detection of road surface defects.
2. Comparison of the accuracy of the proposed road surface defect contour detection method to active contour detection method as well as human drawn contour.
3. Investigation of the limits of the current methods for lateral chromatic aberration reduction, in order to develop a new method to reduce lateral chromatic aberration when using object contour detection in eye fundus images that would not require the camera used to capture the image.

4. Comparison of the accuracy of the new lateral chromatic aberration reduction method, which is presented in this thesis and is based on blood vessels' detection, to methods that are based on using calibration patterns.

1.5 Research methods

The tasks stipulated in the dissertation are solved by analytical and experimental methods. For the analysis of the scientific and experimental results in the fields of chromatic aberration reduction and object contour detection, literature research, systematization, analysis and generalization are used.
Based on the experimental research method, a statistical analysis of the data and the research results is carried out, the generalization method is used to evaluate the results.

1.6 Scientific contribution of the research

The following scientific contribution is presented in the dissertation:

1. A road surface defect contour detection method is developed. The method can detect a contour of a complex, closed object, without uniform texture or with a high color variance – thus it can be applied to road surface defect detection or timber knot contour detection.
2. When comparing the proposed road surface defect contour detection method to an active contour method while using the adaptive threshold, the proposed road surface defect detection method performed on average 25% more accurately.
3. A new method for lateral chromatic aberration reduction in eye fundus images was created, which is based on blood vessels' recognition.
4. A new lateral chromatic aberration reduction in the eye fundus image method was created, which is based on blood vessels' detection and does not require the camera used to take the image. This method is as accurate as other lateral chromatic aberration reduction methods that require calibration patterns.

1.7 Practical value of the research

A road surface defect contour detection method and software was developed. This method is able to detect a complex closed contour, a contour without uniform texture, with a high level of color variance and different contour forms. Practically, this method can be applied in the road industry – road defect detection; or the furniture industry – timber knot contour detection.

A new lateral chromatic aberration reduction in the eye fundus image method was developed. This method is based on blood vessels' detection by appropriately developed software. This method can be applied to various portable eye fundus cameras, where lateral chromatic aberration appears. Lateral chromatic aberration reduction in the eye fundus image method was tested using a SmartScope M5 Optomed camera. The method partially eliminated lateral chromatic aberration and enhanced the image contrast.

1.8 Statements to be defended

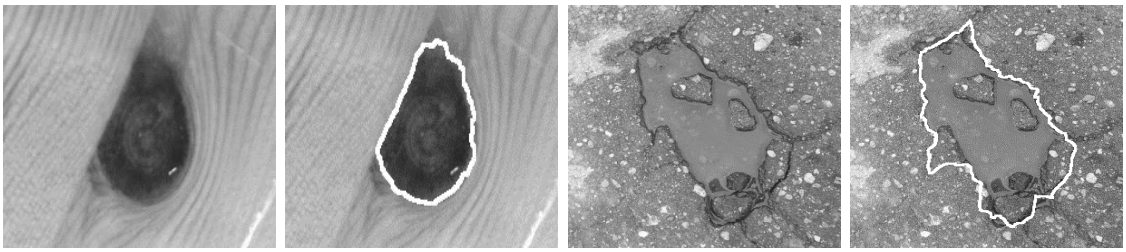
1. The proposed road surface defect contour detection method can be applied in detecting complex and closed contours.
2. The created road surface defect contour detection method is more accurate than the active contour method.
3. The pattern-based lateral chromatic aberration reduction method with the projective model for the reduction of the lateral chromatic aberration effect in eye fundus images is better than the same method with affine, simple and radial models.
4. The developed lateral chromatic aberration reduction method using blood vessels' detection is as accurate as the pattern-based lateral chromatic aberration reduction method.

1.9 Approbation and publications of the research

The main results of the research were published in 9 research papers: two papers were published in periodicals, reviewed scientific journals; two papers were published in conference proceedings; five papers were published in conference abstracts. The main results have been presented and discussed at 4 national and 3 international conferences.

2 Analysis of suitable contour recognition methods for detection of road surface defect contours

There are millions of photographs taken every day, that are used for various applications. Photographs can be categorized into: reflection, emission, absorption, depending on the technology used. Due to the popularity of picture taking, there is high demand for digital image analysis in order to obtain a wide range of information such as: object detection, segmentation, contour recognition etc. Digital image processing is used in many fields: health service, astronomy, meteorology, architecture, forensic investigations, military, manufacturing, engineering and many more. Information is obtained from raster images with low level elements – pixels. Image analysis is a complex task with no universal method that could be applied in the various situations. A variety of methods are used in contour recognition that use neural networks, edge detection operators etc. Unfortunately, these methods are limited due to image noise. Image noise is unnecessary information which needs to be eliminated or reduced as much as possible. However, noise elimination or reduction often results in the loss of contour points and vice versa. Without noise elimination or reduction, noise is recognized as a contour point. Nevertheless, there are contour detection methods immune to noise, such as Snake – Active Contour method and others. On the other hand, these methods have limitations when it comes to images of defects in building wall, road surfaces and more (Figure 1).



a) b) c) d)

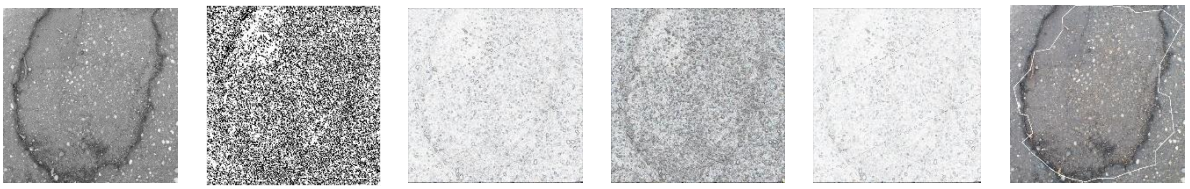
Figure 1. Contours examples a) and c) original images; b) and d) result of method proposed in this paper.

The main problems faced when determining the contour of road surface defects are: no common form of defect; exclusion of unnecessary objects e.g.: water, mud, wells, pavements, shadows etc. It is also difficult to determine accurately the edge of a road surface defect due to cracks in the tarmac. Furthermore, road surface defects do not have a uniform color due to: shadows, weather conditions, under layer color and vice versa.

The literature analysis revealed existing alternative approaches to solve such problems. One of them is using smartphones with accelerometers and global positioning systems. Another approach is the use of pressure sensors built into shock absorbers to detect and quantify the intensity of a pothole. Potholes can also be detected by using: two ultrasonic sensors, laser line striper sensors, ground penetrating radars or hyperspectral imagery etc. Often such methods are not financially viable and require additional equipment. One of the most convenient, well-known and inexpensive ways to recognize road potholes is to use image analysis algorithms that analyze images obtained by a smart device. At present, mobile devices have become an inseparable attribute of our lives. Their technical capabilities allow taking high quality photographs of objects, moreover, mobile networks are able to provide high data transfer rate, so it is practical to create methods capable of measuring parameters of road potholes and upload the collected data for public/personal use of the road companies.

2.1 Detection of road surface defect contour method

An analysis of the contour extraction methods has been accomplished. Such an analysis allowed us to select the best object contour detection method and use it in comparison with our proposed method for pothole contour detection. The Analysis results are presented in Figure 2.



a) b) c) d) e) f)

Figure 2. The result of application of b) Canny, c) Sobel, d) Kirsch, e) Prewitt, f) Snakes algorithms to a pothole image. a) original image.

It can be seen clearly that traditional approaches for contour extraction do not work well and the best result was obtained by applying a segmentation of the Adaptive contour models (snakes). Thus, a new method of road surface defect recognition was recommended and presented in the dissertation see Figure 3.

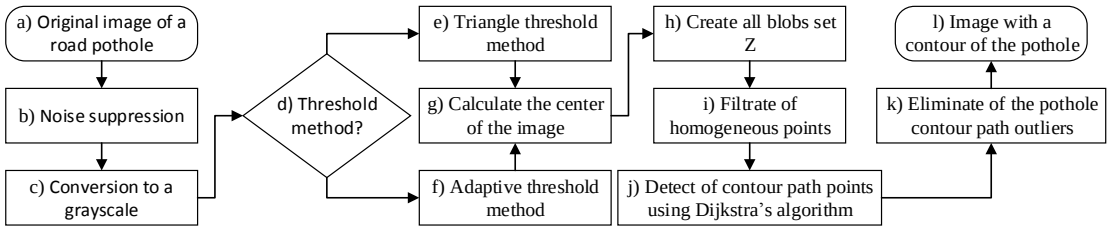


Figure 3. Contour recognition scheme for pothole detection.

Steps of algorithm for this method are as follows:

a) Load of Road surface defect image.

b) *Noise suppression*. Reduction of the image size is accomplished by applying the nearest neighbor interpolation technique.

c) *Conversion to a grayscale*. The resized image is converted to a greyscale.

d) *Thresholding of image for foreground and background segmentation.* In this step, we choose one of the thresholding methods.

e) Triangle threshold method.

f) *Adaptive threshold method.*

g) *Calculate the center of the image C*. We assume that the image center point falls within the area of the pothole (Figure 4).

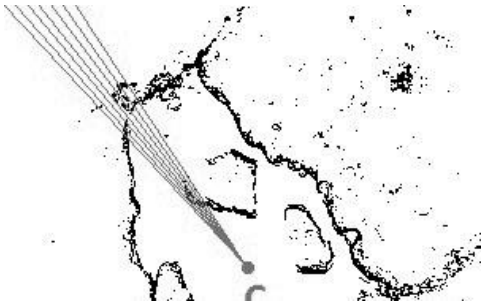


Figure 4. Lines crossing the pothole borders.

h) *Create all blobs set Z*. Drawing the lines from C to each image border point. Figure 4 depicts the line drawing idea. To determine whether the points lay on a line, we have used the Bresenham method. All the lines preserving their order are saved in set Z. Each line (a sample of the line is depicted in Figure 5) can be understood as an ordered list of intensities of black and white pixels. The arrow on the top of the image shows the point ordering direction from the center image point to the image boundary. The line depicts blobs of black pixels. The length D_i of each blob can be obtained by finding the length of the consequent black pixel count.

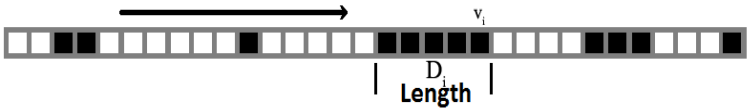


Figure 5. Example of a line in set $\boldsymbol{A}$.

i) *Filtering of homogeneous points*. Since all the lines start from the center C, there are a lot of the same blobs in different lines. With a view to eliminate them, each point that belongs to the line is considered. The coordinates of repeating points are removed from all the lines except the middle ones. Thus, a new set Z is obtained.

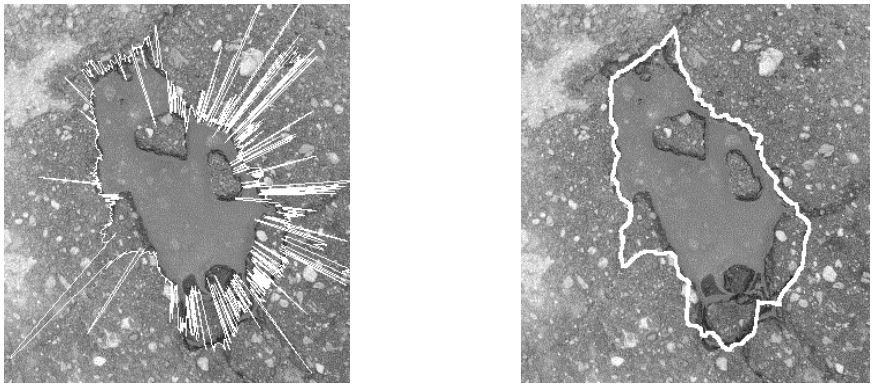
j) *Detection of the contour points using Dijkstra's algorithm*. Detection of the pothole contour path points is performed by Dijkstra`s algorithm with the structure $S = (G, L)$ defined. The graph $G = (V, E)$ is constructed, where $V = \{v_i\}$ is composed of vertices v_i, that are taken from the set Z^* and are presented by each line each blob the furthest black pixels (Figure 5), E consists of edges that connect all the vertices between two neighboring lines. $L = \{l_{ij}\}$ is a set of lengths between the ith and jth vertices of set V. The lengths are calculated by the proposed (1) formula.

$$l_{ij} = w_1(D_i + D_j) + w_2 d_{ij} + w_3(d_{ic} + d_{jc}), \quad (1)$$

where D_i, D_j are lengths of line sections i and j; d_{ij} is the Euclidian distance between the vertices i and j; d_{ic}, d_{jc} are Euclidian distance between the vertex and image center; w_1, w_2, w_3 are weights such as $\sum_{i=1}^{3} w_i = 1$. All the vertices compose an ordered set $F = \{v_i\}$. The weights w_i are selected so as to fit the line to the contour. After a careful analysis, the weights were selected experimentally: $w_1 = 0{,}6$; $w_2 = 0{,}25$; $w_3 = 0{,}15$. The result is presented in Figure 6 left side.

k) *Elimination of the pothole contour path outliers*. A new set $F^* = \{f_i\}$ is constructed from vertices of the set F. At the beginning, we take the first vertex v_0 from the set F and insert it into set F^*, i.e. $f_0 = v_0$. We make an assumption that the vertex v_0 is not an outlier. Then if it is closest to v_0 from 10 left-sided neighbors in set F, we insert the vertex v_i into set F^*. Then, we take the newly obtained vertex as a reference and start to look for its closest neighbour. The process continues until the whole set F is checked.

l) *Image with a contour of the pothole.* The result is shown in Figure 6.

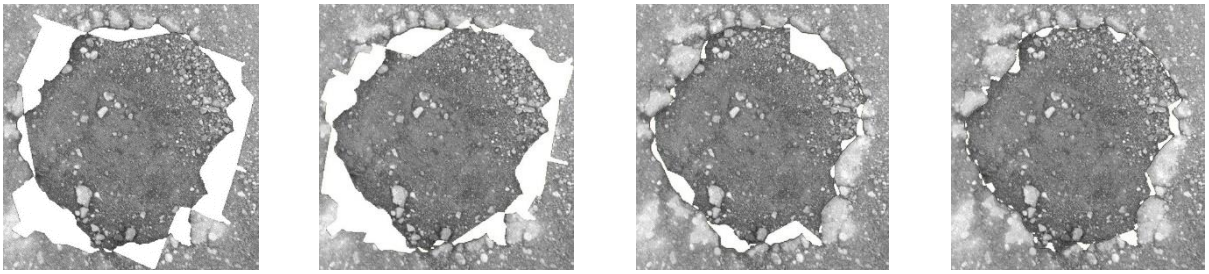


a) b)

Figure 6. a) Contour path after application of Dijkstra's algorithm; b) Smoothed contour of the pothole after filtering procedure.

2.1 Experimental evaluation of road surface defect contour detection methods

Experiments were done by using a set of 105 various resolution images, purposely gathered for the research and captured with a mobile device camera. The aim of the experiment was to evaluate the accuracy of the method for pothole contour detection we have proposed, and that of the snakes method by comparing them to that of the human-drawn pothole contour.



a) b) c) d)

Figure 7. Road surface defect contour detection by different methods: a) Snakes - Triangle; b) Snakes - Adaptive; c) Proposed - Triangle; d) Proposed - Adaptive.

The accuracy was expressed by using (2) formula.

$$C = \begin{cases} \frac{B-A}{B} * 100\%, & B - A > 0 \\ 0, & B - A \leq 0 \end{cases}, \quad (2)$$

where A is the area (white color) of contour calculated applying either the proposed method or snakes method and human-drawn contour; B is the area of a human-drawn contour (Figure 7). The results are shown in Table 1.

Table 1. The accuracy of pothole contour detection methods.

Method	C=(B-A)/B*100%										Average
	100% - 90%	90% - 80%	80% - 70%	70% - 60%	60% - 50%	50% - 40%	40% - 30%	30% - 20%	20% - 10%	10% - 0%	
Snakes - Triangle	2	7	18	15	20	13	6	7	4	9	52%
Snakes - Adaptive	3	10	11	25	11	13	11	4	2	11	53%
Proposed - Triangle	13	25	25	16	11	4	2	0	1	4	70%
Proposed - Adaptive	**15**	**38**	**25**	11	9	2	0	0	0	0	**78%**

When comparing the Snakes-Adaptive and Proposed-Adaptive methods, the better performance is shown by the Proposed-Adaptive method. It increase the difference accuracy by 25%. The highest concurrence (applying the Adaptive threshold and the proposed edge detection method) of the contour drawn when applying the proposed pothole contour detection method and the human-drawn contour was 97%. The lowest accuracy was 42%, mostly as a result of insufficient lighting conditions or external impediments. 15 images were recognized with a size accuracy of $90\% - 100\%$, 38 images with a size accuracy of $80\% - 90\%$, and only 2 images with that of $40\% - 50\%$ or below.

3 Aberration and image quality

In recent years digital image resolution increased dramatically as a result of improvements made to sensors of digital cameras. As a result, aberration effects: blur and additional colors became more visible. Optical system aberrations are divided into: Monochromatic aberration and Chromatic aberration. Monochromatic aberration is divided into: Astigmatic, Comatic, Field curvature, Distortion and Spherical aberrations. Chromatic aberration is divided into: Lateral or Transverse and Axial or Longitudinal Chromatic aberrations.

Monochromatic aberrations are not investigated in this research. Chromatic aberrations can be reduced in two ways: mechanically – adding additional lenses to the optical system; programmatically – applying various methods to correct the digital image by reducing aberrations. Mechanically, chromatic aberration can be reduced by using achromatic, apochromatic or diffractive lenses. However, the production of such lenses is expensive, complicated and also occupies additional space in the device. In order to avoid mechanical limitations there is a variety of programmatical methods proposed. Programmatically, chromatic aberration can be reduced by applying various methods such

as: active lens method; camera calibration using calibration patterns with different correction models; contour detection etc.

Ophthalmologists are often facing problems caused by aberration. Stationary and expensive eye fundus cameras are fitted with achromatic, apochromatic and diffractive lenses systems in order to reduce chromatic aberration. Most portable eye fundus cameras do not have lenses systems that reduce chromatic aberration. Since ophthalmologists get important information from the eye fundus image, having a low quality image makes it more difficult to detect symptoms. The chromatic aberration effect is visible in Figure 8 left image. The image is taken using a Optomed SmartScope M5 eye fundus camera without achromatic, apochromatic or diffractive lenses. It is clear that the blood vessels are blurry, the optic nerve disc boundary is blunt and unnecessary colors occur. Figure 8 right image illustrates an example without chromatic aberration.

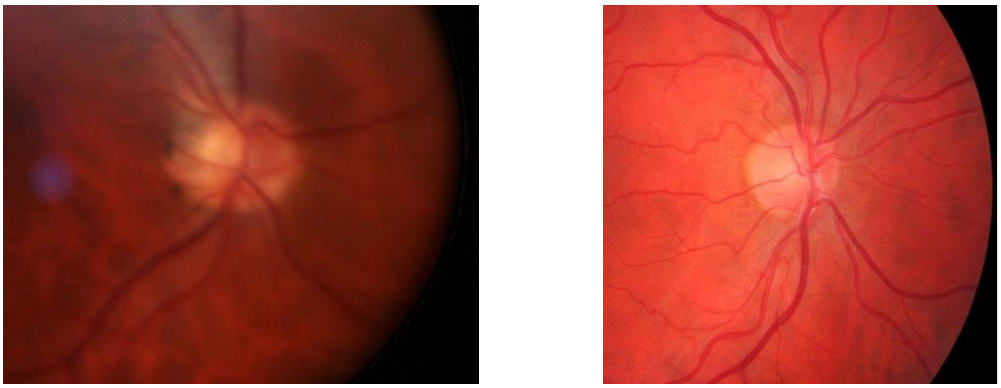


Figure 8. Eye fundus images. Left – image with chromatic aberration. Right – image without chromatic aberration.

The SmartScope M5 Optomed is the camera used for this research. It is clear that when taking images with the camera the chromatic aberration effect appears. Thus, to determine its kind, a chess board or round circle image patterns are used in Figure 9 left. Having these patterns is enough to determine the type of chromatic aberration, since chromatic aberration creates a colorful image after light passes through the optical lens system. That is why colors appear next to squares in the chessboard image. After capturing the selected patterns with the SmartScope M5 Optomed camera, the results in Figure 9 on the right side show that this camera has lateral chromatic aberration.

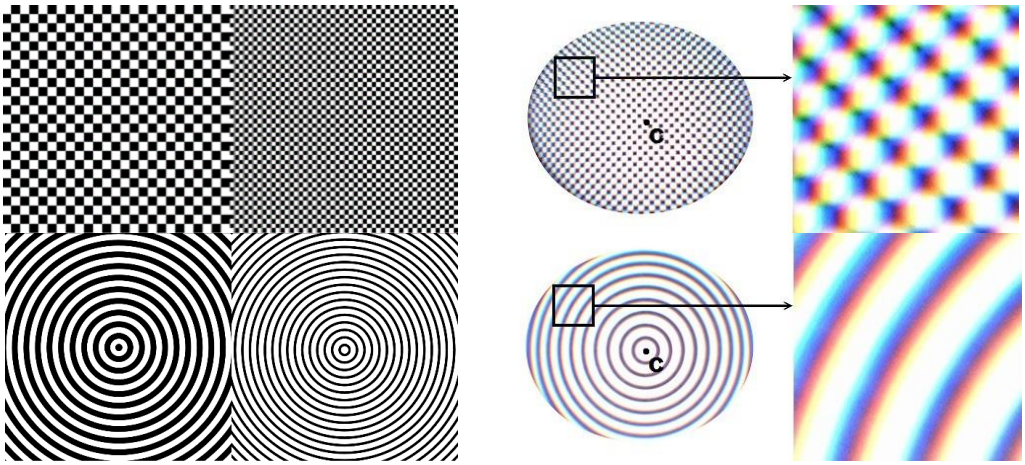


Figure 9. Calibration patterns. From left to right: the original calibration patterns; the patterns captured by the SmartScope M5 camera.

This problem can be solved programmatically; however, there is no universal method to solve this problem for all optical systems and to reduce a variety of distortions. That is why this problem can only be solved separately for each optical system. When there is no information about how an image appears without lateral chromatic aberration after taking it with an Optomed SmartScope M5 camera, then image quality evaluation metrics Blur Metric (M_{BM}), Chromatic Zipper (M_{ChZ}) and Achromatic Zipper (M_{AChZ}) are used to determine the quality without having a reference image. Where Blur metric is to evaluate the level of blur, Chromatic and Achromatic Zippers are used to evaluate the image quality by looking for pixel color differences within similar color pixels nearby.

Since the lateral chromatic aberration effect is a crucial problem, it is clear that it has to be reduced as much as possible by using current or new methods.

4 Lateral chromatic aberration reduction methodology

This chapter describes the methodology used to reduce lateral chromatic aberration in eye fundus images.

4.1 Lateral chromatic aberration reduction methods using calibration patterns and blood vessels' detection

One method used to reduce lateral chromatic aberration in eye fundus images uses calibration patterns. Since this method can only be used when having an eye fundus camera, the research presented a new method based on detection of eye fundus blood vessels, which can be used when only eye fundus images are present. Both methods are described below.

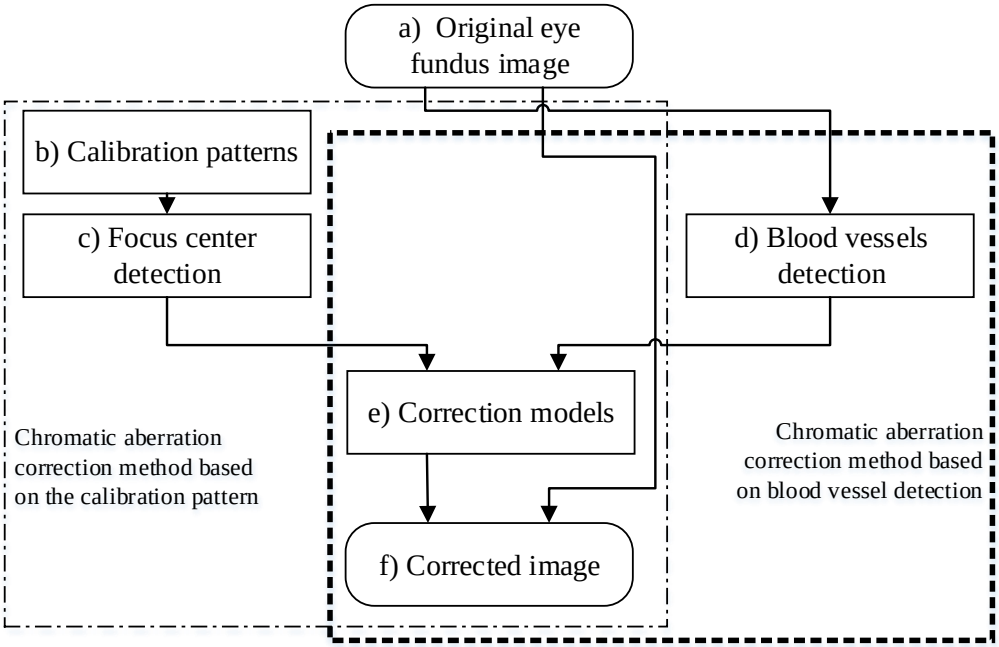


Figure 10. Lateral chromatic aberration correction methods' schema using calibration pattern and blood vessels' detection.

Figure 10 in chain type surrounded part lateral chromatic aberration correction method based on the calibration pattern scheme and stages are as follows:

a) *Original eye fundus image.* Initial eye fundus image is used.
b) *Calibration patterns.* Since this method is based on the calibration of the camera, after conducting experimental testing, a chess board and circle patterns (Figure 9 left side) were chosen.
c) *Focus center detection.* In order to accurately reduce lateral chromatic aberration, the aberration focus center is detected.
d) *Correction models.* Correction models are applied to change the channels of two colors in order to align them to the third color channel. Often, the green channel is used as a reference, the red channel needs to be contracted and the blue channel expanded. This is performed in order to minimize calibration models.
e) *Corrected image.* The result image is achieved by applying a chosen calibration model with the best coefficients on the initial eye fundus image.

Figure 10 in sroke type surrounded part lateral chromatic aberration correction method based on the blood vessels' detection scheme are as follows:

a) *Original eye fundus image.* Initial eye fundus image is used.
b) *Blood vessels' detection.* To avoid using calibration patterns, the eye fundus image is used to detect blood vessels in each color channel.
c) *Correction models.* Correction models are applied in order to alter two color channels of the eye fundus blood vessels' intensiveness, so that they align to a third color channel. Often, the green channel is used as reference, the red channel

needs to be contracted and the blue channel expanded. This is performed in order to minimize calibration models.

d) *Corrected image.* The result image is achieved by applying a chosen calibration model with the best coefficients on the initial eye fundus image.

4.2 Lateral chromatic aberration correction method using calibration patterns

Lateral chromatic aberration correction method using calibration patterns (CP) is conducted in stages as stated in Figure 11.

a) *Original eye fundus image.* Eye fundus image is used see Figure 18 a).

b) *Calibration patterns.* Calibration patterns are captured with a camera and used.

c) *Focus center detection.* Lateral chromatic aberration focus center (x_f, y_f) detection.

d) *Correction models.* Five different correction models are used with the following formulas (4) (5) (6) (7) (8), to correct the red and blue channel intensity in order to align them to the green channel intensity.

e) *Image correction.* To conduct image correction, correction model coefficients $a_0, \ldots, a_7$ are calculated by minimizing RMSE (3) formula, using Levenberg–Marquardt algorithm where $A(x, y)$ is the green channel intensity and $P(x, y)$ are the blue or red channel intensities, w – image width, h – height.

$$\mathrm{RMSE} = \sqrt{\frac{1}{wh}\sum_{x=0}^{w-1}\sum_{y=0}^{h-1}(A(x,y) - P(x,y))^2}, \tag{3}$$

f) *Image outcome.* Image outcome is achieved.

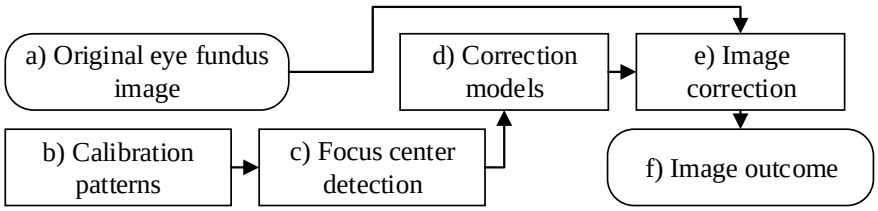


Figure 11. Scheme of lateral chromatic aberration reduction using calibration pattern method.

Since the CP method cannot be used for eye fundus images without having the camera, thus, a new lateral chromatic aberration correction model using blood vessels' detection is presented in this thesis. The new method of correction of lateral chromatic aberration uses blood vessels' recognition, that do not require prior camera calibration, as discussed in the next chapter.

4.3 Determining the best performing lateral chromatic aberration reduction model using calibration patterns

The purpose of this experiment is to determine which model is performing best in the reduction of lateral chromatic aberration in eye fundus images using the CP method

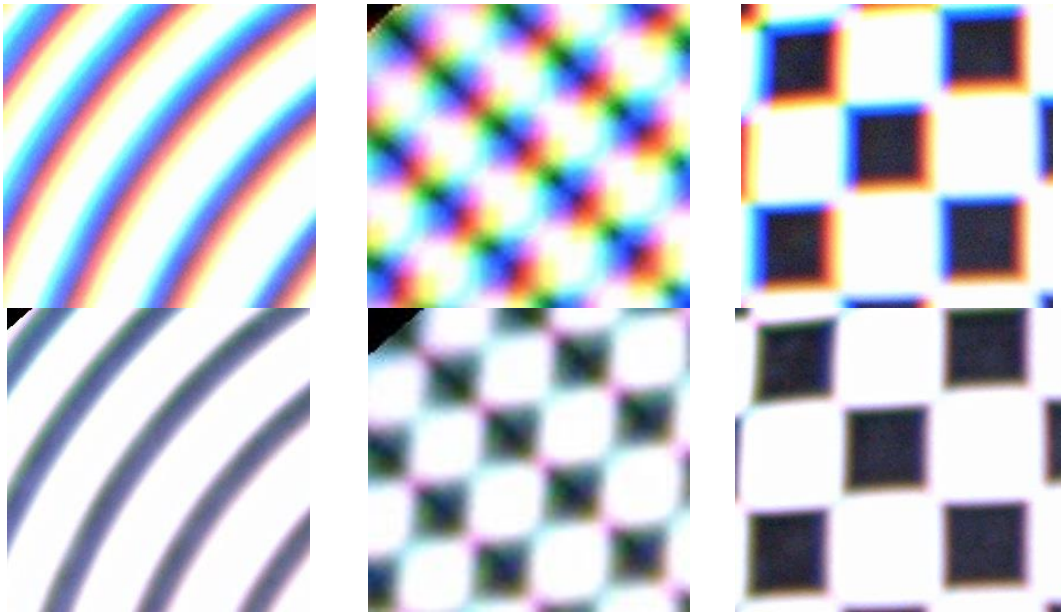


Figure 12. Patterns before (top row) and after (bottom row) the projective correction. From left to right: pattern of circles, chessboard with a square size of 4x4 pixels and a chessboard with the square size of 8x8 pixels.

For using the CP method, two types of calibration patterns are enough to detect lateral chromatic aberration. A chess board is used as a calibration pattern image as seen in Figure 9 left. The Calibration pattern resolution is $20{,}34$ pixels in a square centimeter. The camera is fitted with a 5 megapixel CMOS image sensor. Images were saved in JPG format at a resolution of 1920×1440 pixels.

Calibration patterns were captured using the SmartScope M5 Optomed portable eye fundus camera, $8cm$ away from the lens. The standard adult eye focal distance (image projection on the retina) is $PF' \approx 22mm$ and the distance from camera to eye lens is $FP \approx 18mm$, see Figure 13. Thus, the eye lens was captured from $4cm$ distance to the camera lens. See Figure 13.

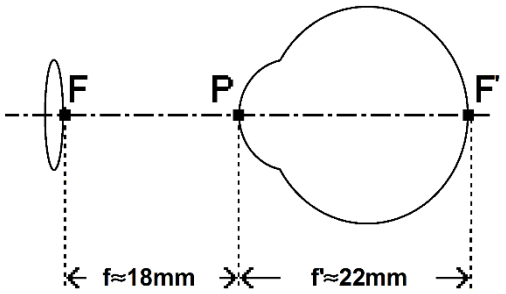


Figure 13. Distance from camera lens to eye retina.

Since the distance between the camera lens and the eye is $4cm$ and the distance between the calibration pattern and the camera lens is $8cm$, all correction coefficients must be 50% lower.

Five different correction models are used to reduce the lateral chromatic aberration in images captured with the SmartScope M5 Optomed portable camera:

- Simple, using a_0, a_1, a_2 coefficients in (4) formula;

$$x' = a_0(x - x_f) + a_1; y' = a_0(y - y_f) + a_2, \tag{4}$$

- Affine, using six $a_0, \dots, a_5$ coefficients in (5) formula;

$$\begin{aligned} x' &= a_0(x - x_f) + a_1(y - y_f) + a_2; \\ y' &= a_3(x - x_f) + a_4(y - y_f) + a_5, \end{aligned} \tag{5}$$

- Projective, using eight $a_0, \dots, a_7$ coefficients in (6) formula;

$$\begin{aligned} x' &= \frac{a_0(x - x_f) + a_1(y - y_f) + a_2}{a_6(x - x_f) + a_7(y - y_f) + 1}; \\ y' &= \frac{a_3(x - x_f) + a_4(y - y_f) + a_5}{a_6(x - x_f) + a_7(y - y_f) + 1}, \end{aligned} \tag{6}$$

- Radial, using one a_0 coefficient in (7) formula;

$$\begin{aligned} x' &= (x - x_f) * (1 + a_0 * r); \\ y' &= (y - y_f) * (1 + a_0 * r); \end{aligned} \tag{7}$$

- Radial, using two a_0, a_1 coefficients in (8) formula.

$$\begin{aligned} x' &= (x - x_f) * (1 + a_0 * r + a_1 * r^2); \\ y' &= (y - y_f) * (1 + a_0 * r + a_1 * r^2); \end{aligned} \tag{8}$$

The green channel is used as a template. All models were calculated for red and blue channels separately, minimizing RMSE using (3) formula by using the Levenberg-Marquardt algorithm. Minimizing is stopped after 100 intentions or if a calculation error is $\varepsilon < 0{,}001$.

To conduct the experimental research, the software was designed using C++ programming language and OpenCV library.

Table 2. Results of correction models using the CP method.

Pattern	Without correction		Simple	Affine	Projective	Radial 1	Radial 2
Circle size of 4x4 pixels	$E_{abr_wc}(G,B)$= 45,26	$E_{abr}(G,B)$	21,65	21,21	**21,18**	28,31	24,47
		$E_{abr_wc}(G,B)/E_{abr}(G,B)$	2,09	2,13	**2,14**	1,60	1,85
	$E_{abr_wc}(G,R)$= 46,53	$E_{abr}(G,R)$	14,57	13,65	**13,65**	23,87	17,87
		$E_{abr_wc}(G,R)/E_{abr}(G,R)$	3,19	3,41	**3,41**	1,95	2,60
Chessboard with square sizes of 4×4 pixels	$E_{abr_wc}(G,B)$= 59,01	$E_{abr}(G,B)$	22,54	22,48	**22,48**	35,49	29,12
		$E_{abr_wc}(G,B)/E_{abr}(G,B)$	2,62	2,63	**2,63**	1,66	2,03
	$E_{abr_wc}(G,R)$= 51,55	$E_{abr}(G,R)$	19,1	19	**18,96**	30,44	21,46
		$E_{abr_wc}(G,R)/E_{abr}(G,R)$	2,70	2,71	**2,72**	1,69	2,40
Chessboard with square sizes of 8x8 pixels	$E_{abr_wc}(G,B)$= 43,01	$E_{abr}(G,B)$	20,07	19,25	**19,25**	28,53	23,76
		$E_{abr_wc}(G,B)/E_{abr}(G,B)$	2,14	2,23	**2,23**	1,51	1,81
	$E_{abr_wc}(G,R)$= 37,24	$E_{abr}(G,R)$	12,98	12,86	**12,86**	20,16	13,19
		$E_{abr_wc}(G,R)/E_{abr}(G,R)$	2,87	2,90	**2,90**	1,85	2,82

In Table 2 E_{abr_wc} is calculated RMSE without using a correction model on the patterns. For pattern examples see Figure 12 top row. E_{abr} is calculated RMSE of image after correction model application. The best results are achieved by the projective model, see Figure 12 bottom row. It is clear that the lateral chromatic aberration decreased significantly. The best result for the blue channel is $2{,}14$ and for the red channel $3{,}41$, on both occasions the average dispersion is lower than $0{,}001$. The Projective model RMSE results are $(33-37\%)$ better than the radial model with one parameter and $(13-18\%)$ better than the radial model with two parameters. Nevertheless, the projective model is only slightly better $(0-0.09\%)$ than the affine model and $(0{,}48-3{,}83\%)$ than the simple model. Affine or simple models may be chosen if calculation speed is required.

4.4 Proposed lateral chromatic aberration correction method for blood vessels' detection

The new method of correction of lateral chromatic aberration using blood vessels' recognition (BD method) proposed in the thesis is carried out in the following stages, as shown in Figure 14:

a) *Original eye fundus image.* Eye fundus image is used, see Figure 18 a).
b) *Blood vessels' detection.* Eye fundus blood vessels are detected in each RGB channel. The eye fundus blood vessels' detection method is widely described in chapter 4.6.
c) *Correction models.* Five different correction models are used with the following formulas (4) (5) (6) (7) (8), to correct the red and blue channel intensities in order to align them to the green channel intensity.
d) *Image outcome.* To conduct the image correction, correction model coefficients $a_0, \dots, a_7$ are calculated by minimizing RMSE (3) formula, using the Levenberg–

Marquardt algorithm where $A(x, y)$ is the green channel intensity and $P(x, y)$ are the blue or red channel intensities, w – image width, h – height.

e) *Corrected image.* Image outcome is achieved.

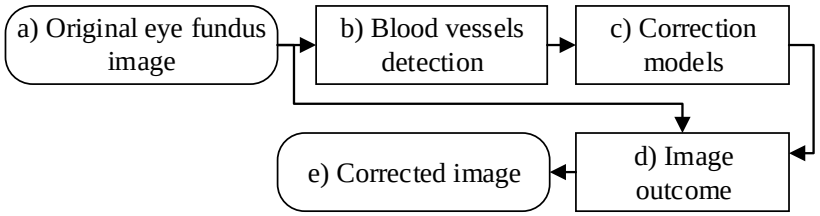


Figure 14. Scheme of lateral chromatic aberration reduction using blood vessel method

4.5 Lateral chromatic aberration focus center detection

Because the lateral chromatic aberration center is important for adjusting the lateral chromatic aberration as accurately as possible and it is not usually located at the center of the image due to the various complex lens systems, it is necessary to determine it.

Some of the methods for determining the focus center of the lateral chromatic aberration are easily found in the literature. To set up the focus center for lateral chromatic aberration Hartley and Kang offered a method for identifying lines by taking multiple images at different angles, Wighton and others suggested using circle or square pattern images.

Since this research uses square patterns and only one image, Wighton and other lateral chromatic aberration focus center detection method (FCT) was chosen. The focus of this method is to find the center of each circle or square in each channel. After finding the center of a square or a circle, we get three points through which the straight line is drawn in each channel. After selecting the straight lines for each square or circle, the focus center of the lateral chromatic aberration is found in the center of the straight line. The FCT method steps are as follows:

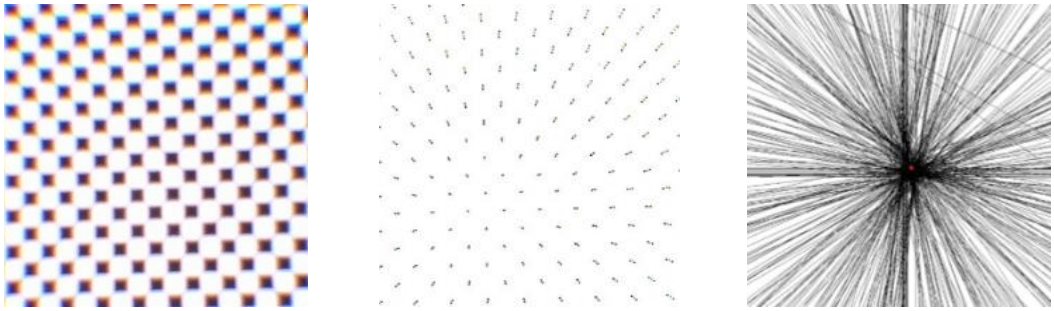
1. *Calibration patterns.* Chess board calibration patterns used are shown in Figure 9 left side.
2. *The center of the photo is determined.* The image taken with the camera has an elliptical contour, which is always the same and the axes are parallel to the edges of the image. Horizontal and vertical scans are used to find elliptic axis lengths and to calculate the elliptical center.
3. *A square.* A square is made $l \times l$ in the center of the image, see Figure 15 a). The square's side length is $l = \sqrt{2} * a_l$, where a_l – half line of short elliptical axis.
4. *Centers are identified in each RGB channel.* In Figure 15 b) it is clear that some RGB channels are further away from each other, than others. This is highly visible on the sides of the image.
5. *A line is drawn for each square*. Shown in Figure 15 c) the lateral chromatic aberration focus center is a point (x_f, y_f), that is generated by minimizing the total sum of each line by using (9) formula.

$$(x_f, y_f) = argmin_{x,y} \sum_{i=1}^{N} d_i(x,y)^2, \quad (9)$$

where $d_i(x,y)$ is the distance from point (x,y) to the i-th line (a_i, b_i, c_i). The center was calculated using *perpendicular linear regression* when (a_i, b_i, c_i) are known. x_f is calculated by (11) formula, but y_f is calculated by (10) formula.

$$y_f = \frac{\sum_{i=1}^{N} b_i c_i \sum_{i=1}^{N} a_i^2 - \sum_{i=1}^{N} a_i c_i \sum_{i=1}^{N} a_i b_i}{(\sum_{i=1}^{N} a_i b_i)^2 - \sum_{i=1}^{N} a_i^2 \sum_{i=1}^{N} b_i^2}; \quad (10)$$

$$x_f = \frac{-y_f \sum_{i=1}^{N} a_i b_i - \sum_{i=1}^{N} a_i c_i}{\sum_{i=1}^{N} a_i^2}. \quad (11)$$



a) b) c)

Figure 15. Lateral chromatic aberration focus center: a) Photograph of a pattern; b) RGB channel centers of each square; c) Lines drawn through each RGB channel center.

The FCT method finds only one common lateral chromatic aberration focus center. Since the lateral chromatic aberrations are reduced in two channels, i.e. the red color channel is compressed and the blue color channel is expanded, the lateral chromatic aberration focus center has to have two and detect two.

The FCK method to detect two lateral chromatic aberration focus centers is presented in this dissertation. Firstly, one channel is chosen as a reference channel. The green channel was chosen, since the green color wave length is ($\sim 520 - 570\ nm$), which is in the middle between red ($\sim 620 - 740\ nm$) and blue ($\sim 450 - 495\ nm$). Also, the Optomed SmartScope M5 camera with a Bayer filter was used, which has mostly green color filters, and therefore the green color channel appears to be more visible and is focused better. Since reducing lateral chromatic aberrations requires the red color channel intensity to be deducted from the green color channel intensity (G-R) and the blue color channel intensity deducted from the green color channel intensity (G-B), two focus centers (G-R) and (G-B) are detected. The dissertation suggests the following FCK method algorithm steps:

1. *Calibration patterns.* A chess board calibration pattern is used. See Figure 9 left.
2. *Intensity subtraction in channels.* In order to see aberrations, the intensity of the red channel has to be subtracted from the green channel. The result is the intensity difference (G-R) shown in Figure 16 a). It is clear, that the edges of the generated image have obvious differences. However, the differences are less significant around the center of the generated image. A similar technique was first applied by

Luhman.

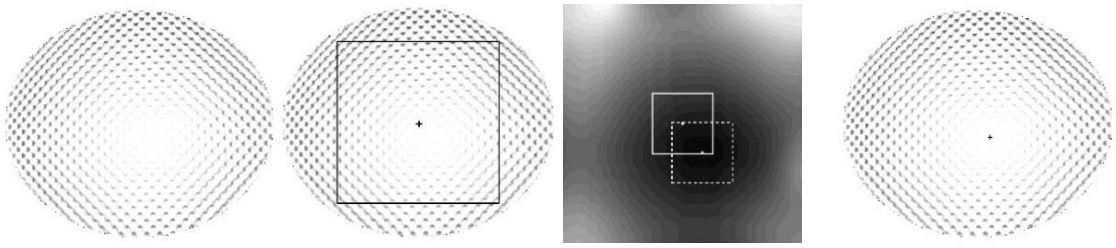
3. *Image center*. The image center is determined (x_c, y_c). The image captured with the camera has elliptic contours, which are always the same, also axes are parallel to the edges. Horizontal and vertical scans are used to find the elliptic axle length and to calculate the elliptic center.
4. *A square*. A square is made $l \times l$ in the center of the image, see Figure 16 b). The square's side length is $l = \sqrt{2} * a_l$, where a_l – half line of short elliptical axis. Gaussian blur is applied by using (12) formula with standard deviation $\sigma = 64$ in order to achieve a smooth image as seen in Figure 16 c).

$$G_f(x, y) = \frac{1}{2\pi\sigma^2} * e^{-\frac{x^2+y^2}{2\sigma^2}}, \tag{12}$$

where σ – standard deviation, (x, y) –image pixel coordinates.
Function (13) is used to find G-R focus center $(\mathrm{x_f}, \mathrm{y_f})$. This function is minimized by using the Quasi-Newton method. A starting position (white square) and a new G-R focus center (striped square) can be seen in Figure 16 c). The focus center of the final lateral chromatic aberration G-R (x_f, y_f) can be seen in Figure 16 c)

$$F(x_f, y_f) = \sum_{x=\left[-\frac{l}{8}\right]}^{\left[\frac{l}{8}\right]} \sum_{y=\left[-\frac{l}{8}\right]}^{\left[\frac{l}{8}\right]} I(x + x_f, y + y_f), \tag{13}$$

where l – size of a square made, $I(x, \mathrm{y})$ – pixel intensity (x, y), (x_f, y_f) – focus center point of aberration.



a) b) c) d)

Figure 16. Lateral chromatic aberration focus center detection in G-R

The experimental research conducted showed that the FCK method used for detecting two lateral chromatic aberration focus centers – performed calculations 17 times quicker as well as detected a lateral chromatic aberration center with similar performance in comparison to the FCT method.

4.6 Comparison of lateral chromatic aberration focus center detection methods

The aim of this experiment is to determine which lateral chromatic aberration focus center detection method is more accurate and quicker. Two methods are examined: the commonly used method using object centers in each channel (FCT) and the method

proposed in this dissertation, that is seeking for each channel minimal differences of intensities (FCK).

A chess board is used as a calibration pattern image as seen in Figure 9 left. The calibration pattern resolution is 20,34 pixels per square centimeter. These calibration patterns were captured using a SmartScope M5 Optomed portable eye fundus camera, 8 *cm* away from the lens. The camera was fitted with a 5 megapixel CMOS image sensor. Images are saved in JPG format at a resolution of 1920×1440 pixels. The experiments were conducted using projective modes, because they performed best in terms of reduction of lateral chromatic aberration. Equipment used for the experiments: Windows 8.1 operating system with Intel i7-550U, 2,40GHz processor, 8GB RAM, C++ programing language with OpenCV library.

Table 3. Results of correctional models using CP method.

Method	Without correction		Projective model	Time
Using image center	$E_{abr_wc}(G,B)$= 59.01	$E_{abr}(G,B)$	26,44	0s
		$E_{abr_wc}(G,B)/E_{abr}(G,B)$	2,23	
	$E_{abr_wc}(G,R)$= 51.55	$E_{abr}(G,R)$	20,80	
		$E_{abr_wc}(G,R)/E_{abr}(G,R)$	2,48	
FCT	$E_{abr_wc}(G,B)$= 59.01	$E_{abr}(G,B)$	22,48	42,55s
		$E_{abr_wc}(G,B)/E_{abr}(G,B)$	2,63	
	$E_{abr_wc}(G,R)$= 51.55	$E_{abr}(G,R)$	18,96	
		$E_{abr_wc}(G,R)/E_{abr}(G,R)$	2,72	
FCK	$E_{abr_wc}(G,B)$= 59.01	$E_{abr}(G,B)$	22,49	2,44s
		$E_{abr_wc}(G,B)/E_{abr}(G,B)$	2,62	
	$E_{abr_wc}(G,R)$= 51.55	$E_{abr}(G,R)$	18,98	
		$E_{abr_wc}(G,R)/E_{abr}(G,R)$	2,72	

Table 3 shows that both methods detected the lateral chromatic aberration focus center almost equally. Also, it is clear that when using the image center instead of the lateral chromatic aberration focus center, RMSE underperformed by ~ 12% in comparison to the lateral chromatic aberration focus center detection methods. The method proposed in this dissertation underperformed by 0,07% when minimizing RMSE in comparison to the FCT method. However, the FCK method performed calculations quicker than the FCT method by 17 times. The FCT method took longer to perform calculations, due to detecting over 200 object centers in each channel and drawing lines. Theoretically, it is enough to draw two crossing lines to set the lateral chromatic aberration center. This way calculations are performed quicker, but accuracy is decreasing.

4.7 Eye fundus blood vessels' detection

All images contain visible noise and the red color is dominating when using the Optomed SmartScope M5 camera. In order to perform a correction to the lateral chromatic aberration in eye fundus images without using calibration pattern images, certain objects

have to remain in each channel. The remaining objects are used to conduct the lateral chromatic aberration correction. In the case of eye fundus image lateral chromatic aberration correction, these objects are blood vessels.

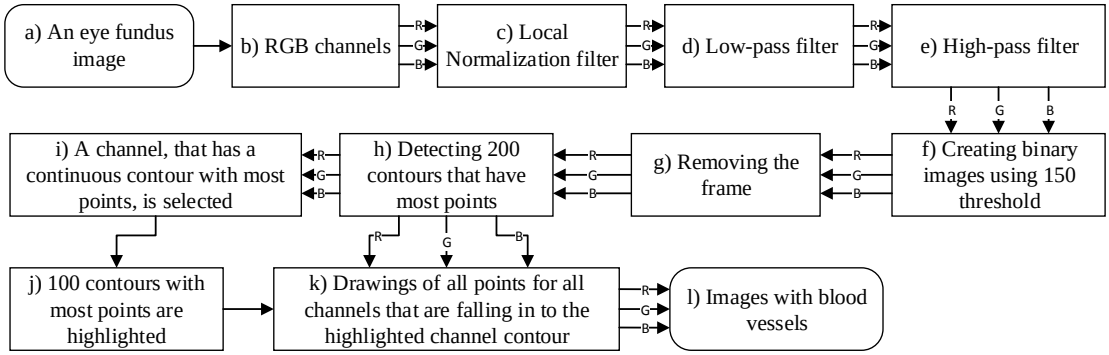


Figure 17. Scheme of blood vessels' detection.

There are a number of methods to identify blood vessels. Large blood vessels are the most important features of the image that show the magnitude of lateral chromatic aberration. Therefore, a large blood vessel identification method was chosen. A schema of the blood vessels' detection algorithm is presented in Figure 17. Blood vessels are detected in each channel from eye fundus images. The steps of the blood vessels' detection algorithm are as follows:

a) An eye fundus image (Figure 18 a)*).*

b) *RGB channels.* This image is split into RGB channels.

c) *Local normalization filter.* A local normalization filter to reduce the difference of illumination is applied to each channel (Figure 18 b)). After the experimental test, the best results were achieved with the parameters $\sigma_1 = 10$ and $\sigma_2 = 20$.

d) *Low-pass filter.* Low-pass filters were used.

e) *High-pass filter.* High-pass filters (Figure 18 c)) were used.

f) *Creating a binary image using 150 threshold.* Binary images were created using threshold 150 (Figure 18 d)).

g) *Removing the frame.* Since the image captured with the camera has an elliptic contour that is always the same and the axes are parallel to edges, all pixels out of the range of the elliptic scope – are eliminated, resulting in the elimination of the frame.

h) *Detecting* 200 *contours that have most points.* 200 continual contours, having the largest number of points were selected.

i) A channel, having a continual contour with most points, was selected.

j) *100 contours with most points are highlighted*, as only the largest blood vessels are important. Blood vessels in diverse channels are located at different locations due to the lateral chromatic aberration, therefore 100 contours with the most points are highlighted to cover the blood vessels in all channels. The pixels are highlighted using the dilate method in OpenCV library Figure 18 e)

k) *Drawing of all points for all channels that are falling into the highlighted channel contour.* Drawings of all points for all channels falling into the highlighted channel contours are given.

l) *Images with blood vessels.* Images with blood vessels in the eye fundus in different RGB channels are visible in Figure 18 f), g) and h).

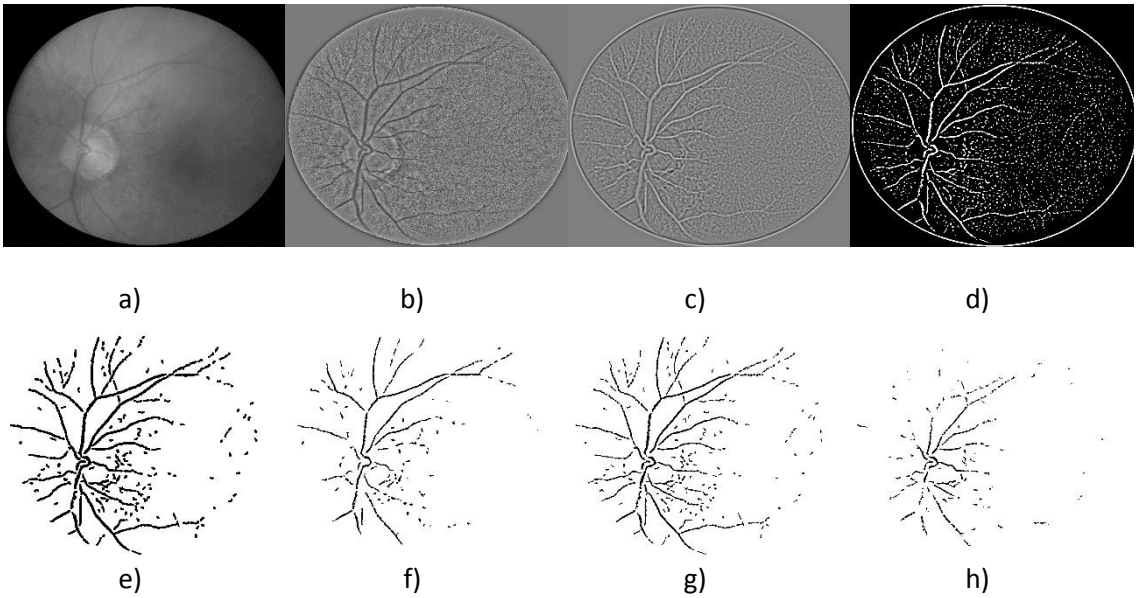


Figure 18. A step-by-step example of blood vessels' detection: a) original image; b) local normalization filter; c) high-pass filter; d) thresholding; e) 100 highlighted contours; f) blue channel contours; g) green channel contours; h) red channel contours.

4.8 Comparison of the lateral chromatic aberration reduction method using calibration patterns and the eye fundus blood vessels' detection

The purpose of this experiment is to compare the accuracy of the lateral chromatic aberration reduction: a method presented in the dissertation, which is based on blood vessels' detection, to a method using calibration patterns.

The Optomed SmartScope M5 was used to take 58 images in order to reduce the lateral chromatic aberration effect. The camera was fitted with a 5 megapixel CMOS image sensor. The images are saved in JPG format at a resolution of 1920×1440 pixels. Experiments were conducted using projective modes, because they performed best in terms of the reduction of lateral chromatic aberration.

There is no information about how the eye fundus image appears without a lateral chromatic aberration after taking it with the Optomed SmartScope M5 camera. Therefore Blur Metric (M_{BM}), Chromatic Zipper (M_{ChZ}) and Achromatic Zipper (M_{AChZ}) metrics are used to determine the quality.

The first line in Table 4 represents the average of metrics in all images without a correction. The second and third lines represent the average of metrics in all images after applying a correction using the CP and BD methods. The results revealed that the quality of images increased after using both methods. Furthermore, the CP method showed slightly better results with all metrics. The dispersion in all metrics is shown in the last three lines of the table. The results make it clear that all dispersions are highly similar.

Table 4. Results of metrics evaluation in lateral chromatic aberration reduction.

	M_{BM}	M_{ChZ}	M_{AChZ}
Mean value using the original images	0,206	14,633	14,387
Mean value using images from the CP method	**0,179**	**13,855**	**14,034**
Mean value using images from the BD method	0,192	13,864	14,083
Dispersion value using the original images	0,00035	0,02411	0,31898
Dispersion value using images from the CP method	0,00050	0,02712	0,42539
Dispersion value using images from the BD method	0,00047	0,02259	0,49019

A Student t-test was performed in order to evaluate the hypothesis of whether the average values are equal prior and after correction. Table 5 shows that when using importance value $p = 0{,}05$, this hypothesis can be rejected, meaning that metric values are significantly different when comparing the original image to the image generated by using the CP method, as well as when comparing the original image to the image generated by using the BD method. Also, it is clearly seen that the Student t-test results show that the averages of the CP and BD methods are significantly different when M_{ChZ} and M_{AChZ} metrics are used, thus, this hypothesis cannot be rejected. However, when using M_{BM} metrics, the differences are meaningless. Even though, when reducing lateral chromatic aberration, the CP method showed slightly better results than the BD method, the BD method can still be used with images without the necessity of having the camera used to take the images.

Table 5. Student t-test results.

	M_{BM}	M_{ChZ}	M_{AChZ}
T-test original image with CP method	3,18E-15	1,78E-22	4,48E-09
T-test original image with BD method	7,94E-10	7,03E-23	9,22E-08
T-test CP method with BD method	3,01E-08	6,55E-01	2,35E-01

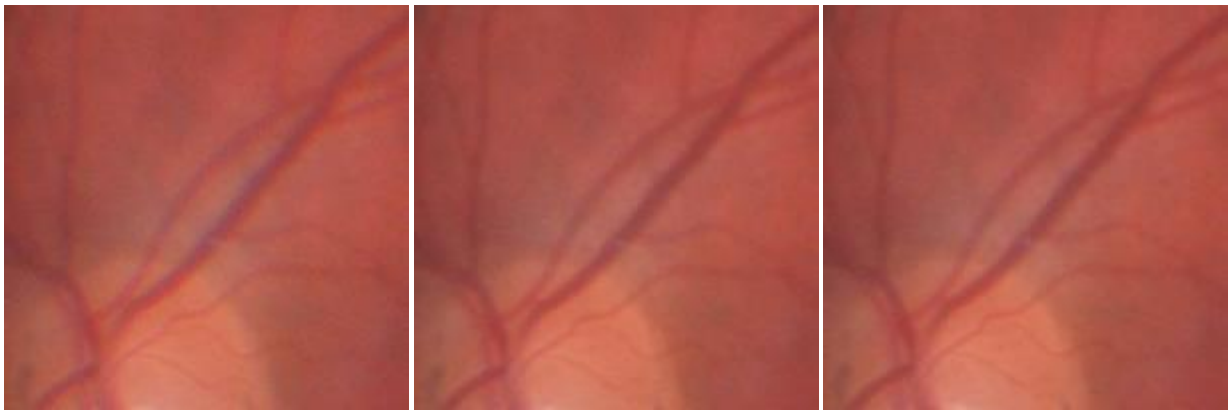


Figure 19. Correction result by means of the CP and BD methods using the projective model. Left column original image. Middle column image using CP method correction. Right column image using BD method correction.

The Figure 19 left image fragment is without correction; the middle image fragment is after the CP method correction application and the right image fragment is after the BD method correction application. It is clearly seen, that after applying either correction, the lateral chromatic aberration was reduced significantly.

5 General conclusions

1. The proposed method to detect road surface defects performs at an average of 78% detection rate when compared to a human defined contour.
2. The proposed road surface defect contour detection method with an adaptive threshold allows a 25% higher accuracy when compared to the active contour method with an adaptive threshold.
3. In order to reduce the lateral chromatic aberration effect in eye fundus images while using calibration patterns based on reduction methods, it is crucial to use the best-performing projective model. Experiments show that the lateral chromatic aberration method based on the projective model, had the best results and the RMSE error decreased an average of 2,14 times in the blue channel and 3,14 times in the red channel. After repeating the experiment 20 times with random initial correction coefficient values in both cases, the average dispersion is lower than 0,001. The worst performance occurred when radial models were used. The RMSE results of the projective model are $(33 - 37\%)$ better than radial with one parameter and $(13 - 18\%)$ better than radial with two parameters. It can be concluded that the projective model is performing slightly better $(0 - 0{,}1\%)$ than the affine model and $(0{,}48 - 3{,}83\%)$ than the simple model. The affine or simple models are better to be used when a higher calculation speed is required.
4. It is safe to say that, to assess the quality of the lateral chromatic aberration reduction after applying Blur metric (M_{BM}), chromatic zipper (M_{ChZ}) and achromatic zipper (M_{AChZ}) metrics – pattern based on the lateral chromatic aberration reduction method with the projective model (CP) as well as the created

lateral chromatic aberration reduction method using blood vessels' detection (BD) – allows to effectively decrease the lateral chromatic aberration effect. Also, the difference between the lateral chromatic aberration reduction method with reference to M_{ChZ} and M_{AChZ} metrics is meaningless. M_{BM} metrics show that, when using the CP method, the image quality increased by 13,1%, when using BD – 6,8%. With reference to the Student t-test, such a difference is important. M_{ChZ} metrics show that when using the CP method, the image quality increased by 5,32%, when using BD – 5,25%. Moreover, M_{AChZ} metrics show that when using the CP method, the image quality increased by 2,45%, when using BD – 2,11%. Since, according to two out of three metrics, the difference between the methods is slight, the BD method can be applied instead of CP, if using pattern images is not an option.

6 List of publications

Articles published in periodical scientific journals:

1. Jakštys V.; Marcinkevičius V.; Tichonov J.; Treigys P. Detection of the Road Pothole Contour in Raster Images. Information Technology and Control. ISSN 1392–124X. 2016. T. 45. Nr. 3. 300–307. Impact factor 0.475.
2. Petkus T.; Tichonov J.; Filatovas E.; Jakštys V. Quality Assessment of High-Resolution Images with Small Distortions after Compression. Baltic journal of modern computing. ISSN 2255-8942. 2017. Vol. 5. Issue. 2. 206–220.

Articles published in other publications:

3. Jakštys V.; Marcinkevičius V.; Treigys P. The Investigation of Chromatic Aberration Correction for Digital Eye Fundus Images. International Congress on Computer Science: Information Systems and Technologies (CSIST'2016). Minsk. Belarus. 2016. ISBN 9789855663691. 1000–1005.
4. Jakštys V.; Marcinkevičius V.; Treigys P. Evaluation of Correction Methods of Lateral Chromatic Aberration in Digital Eye Fundus Images, The 8th International Conference on Pattern Recognition Systems (ICPRS-17). Madrid. Spain. 2017. ISBN 9781785616525. 59–64.
5. Jakštys V.; Marcinkevičius V.; Treigys P. Research on Identification of Defect Contours of Road Surface in Raster Images. Data analysis methods for software systems : 6th International Workshop. Druskininkai. Lithuania. 2014. ISBN 9789986680505. 26.
6. Jakštys V. Metodas kelio dangų defektų kontūrams nustatyti. Fiziniu ir technologijos mokslu tarpdalykiniai tyrimai: penktoji jaunųjų mokslininkų konferencija: pranešimų santraukos. Vilnius. Lithuania. 2015. Lietuvos mokslų akademijos leidykla. 48–51.
7. Jakštys V.; Marcinkevičius V.; Treigys P. Experimental Investigation of Chromatic Aberration Elimination in Digital Images of Eye Fundus Camera. Data analysis methods for software systems : 7th International Workshop. Druskininkai. Lithuania. 2015. ISBN 9789986680581. 26.

8. Jakštys V.; Marcinkevičius V.; Treigys P. Lateral Chromatic Aberration Correction in Digital Eye Fundus Images. EURO 2016: 28th European conference on operational research. Poznań 3-6.07.2016: Conference handbook. Poland. 139–139.
9. Jakštys V.; Marcinkevičius V.; Treigys P. An application of radial distortion models for chromatic aberration correction Data analysis methods for software systems: 8th International Workshop. Druskininkai. Lithuania. 2016. ISBN 9789986680611. 25–26.

7 About the author

Vytautas Jakštys was born in Kudirkos Naumiestis. 2002 studied at Kaunas Technology University. 2010 studied at Vilnius Pedagogical University, achieved Bachelor's Degree in Informatics, with Teaching Certificate. 2013 studied at Lithuanian University of Educational Sciences, achieved Master's degree in informatics. 2013–2018 (planned) PhD () Vilnius university, Institute of Data Science and Digital Technologies.

KONTŪRO ATPAŽINIMO METODŲ TAIKYMAS SKERSINEI CHROMATINEI ABERACIJAI ŠALINTI AKIES DUGNO VAIZDUOSE IR KELIO DANGOS DEFEKTAMS ATPAŽINTI

Tyrimų sritis

Disertacijoje gauti rezultatai susiję su dviem tyrimų sritimis: vaizdų apdorojimu (angl. *Image Processing*) ir vaizdų analize (angl. *Image Analysis*).

Šioje disertacijoje vaizdų analizės ir apdorojimo kontekste tiriami kontūro atpažinimo metodai sprendžiant kelio dangos defektų kontūrų atpažinimo ir skersinės chromatinės aberacijos akies dugno vaizduose sumažinimo uždavinius.

Problemos aktualumas

Literatūroje sutinkamų kontūrų atpažinimo metodų tikslumas labai sumažėja, jeigu vaizdo didelė spalvinė variacija, nevienalytė tekstūrą, jų forma kiekvienu atveju kinta. Šiai grupei vaizdų priskiriami ir tokie vaizdai, kaip medžio šakos lentoje, ištrupėjusios namo sienos dalys, kelio dangos defektai. Kyla poreikis sukurti metodą, kuriuo būtų galima automatizuotai ir tiksliai atpažinti šiuos kontūrus.

Kita disertacijos tiriama sritis, kurioje taikyti kontūrų atpažinimo metodai – skersinės chromatinės aberacijos šalinimas. Šį efektą mechaniškai galima sumažinti achromatiniais, apochromatiniais arba difrakciniais lęšiais. Tačiau jei ribojami fotoaparatų dydžiai, mechaninis sprendimų būdas netinka, nes atsiranda papildomos vietos, svorio ir kaštų ribojimų. Dėl šių priežasčių kyla poreikis kiekvienai optinei sistemai sukurti programinę įrangą, kuri kaip galima labiau sumažintų skersinę chromatinę aberaciją. Literatūroje sutinkamiems metodams, kuriais sumažinama skersinė chromatinė aberacija dažniausiai reikalingas fotoaparatas, su kuriuo fiksuota scena. Kadangi visuose akies dugno vaizduose matomas kraujagyslių tinklas, atpažinus jų kontūrus atsirado galimybė sukurti metodą, kuris nereikalautų fotoaparato, su kuriuo fiksuota scena.

Tyrimų objektas

Disertacijos tyrimo objektas – skaitmeniniai vaizdai, objektų kontūrų atpažinimas, skersinės chromatinės aberacijos šalinimas taikant objektų kontūrų atpažinimą.

Darbo tikslas ir uždaviniai

Darbo tikslas:

Sukurti metodus, grindžiamus objektų kontūro atpažinimo metodais, kurie atpažintų kelio dangos defektų kontūrus ir mažintų skersinę chromatinę aberaciją akies dugno vaizduose.

Šiam tikslui pasiekti sprendžiami tokie uždaviniai:

Atlikti esamų metodų, skirtų didelė spalvinė variacijos ir nevienalytės tekstūros objektų kontūrams atpažinti, analizę ir sukurti metodą, skirtą kelio dangos defektų kontūrams atpažinti.

Palyginti disertacijoje sukurto kelio dangos defektų kontūrų metodo tikslumą su aktyvaus kontūro metodu ir žmogaus apibrėžtais kontūrais.

Atlikti esamų metodų, skirtų skersinei chromatinei aberacijai šalinti analizę ir įvertinti galimybę bei sukurti metodą skersinei chromatinei aberacijai šalinti akies dugno vaizduose be fotoaparato naudojant objektų kontūro atpažinimą.

Palyginti disertacijoje pasiūlyto metodo, kuris grindžiamas kraujagyslių tinklo atpažinimu, skersinės chromatinės aberacijos mažinimo tikslumą su kalibravimo šablonais, grindžiamais skersinės chromatinės aberacijos šalinimo metodais.

Tyrimų metodai

Disertacijoje suformuluoti uždaviniai sprendžiami analitiniais ir eksperimentiniais metodais. Analizuojant skersinės chromatinės aberacijos šalinimo ir objektų kontūrų nustatymo mokslinius straipsnius ir eksperimentinius rezultatus naudoti informacijos paieškos, sisteminimo, analizes ir apibendrinimo metodai.

Mokslinis naujumas

Disertacijoje gauti šie rezultatai:

Sukurtas kelio dangos defektų kontūrų atpažinimo metodas, kuriuo galima atpažinti sudėtingą uždarą nevienalytės tekstūros ir didelės spalvinės variacijos objekto kontūrą, tokį, kaip kelio dangos defektas ar medžio šaka lentoje.

Lyginant pasiūlytą kelio dangos defektų kontūrų atpažinimo metodą su aktyvaus kontūro metodu naudojant prisitaikančio metodo binarizacijos slenkstį nustatyta, kad vidutiniškai 25% tiksliau kontūrą atpažino pasiūlytas kelio dangos defektų kontūrų atpažinimo metodas.

Sukurtas naujas skersinės chromatinės aberacijos šalinimo akies dugno vaizduose metodas grindžiamas kraujagyslių tinklo struktūros atpažinimu.

Sukurtas naujas skersinės chromatinės aberacijos šalinimo akies dugno vaizduose metodas, pagrįstas kraujagyslių tinklo atpažinimu ir nereikalaujantis fotoaparato, tikslumu nenusileidžia kalibravimo šablonais grindžiamiems skersinės chromatinės aberacijos šalinimo metodams.

Praktinė darbo reikšmė

Sukurtas kelio dangos defektų kontūrų atpažinimo metodas ir programinė įranga. Šiuo metodu galima atpažinti sudėtingą uždarą nevienalytės tekstūros, didelės spalvinės variacijos ir skirtingos formos kiekvienam vaizde kontūrą. Praktiškai šį metodą gali taikyti kelininkai kelio dangos defektams atpažinti, baldininkai – šakoms lentoje atpažinti.

Sukurtas naujas skersinės chromatinės aberacijos šalinimo akies dugno vaizduose metodas, kuris yra grindžiamas kraujagyslių tinklo atpažinimu, ir sukurta programinė įranga. Šis metodas gali būti naudojamas įvairioms portatyvinėms akies dugno kameroms, kuriose pasireiškia skersinė chromatinė aberacija. Šis metodas, išbandytas SmartScope M5 Optomed fotoaparatu, vaizduose sumažino skersinę chromatinę aberaciją ir pagerino vaizdų kontrastą.

Ginamieji teiginiai

Pasiūlytas kelio dangos defektų kontūrų atpažinimo metodas yra tinkamas sudėtingam uždaram kontūrui atpažinti.

Sukurtas kelio dangos defektų kontūrų atpažinimo metodas veikia tiksliau už aktyvaus kontūro metodą.

Kalibravimo šablonais grindžiamas skersinių chromatinių aberacijų šalinimo metodas su projekciniu modeliu skersinės chromatinės aberacijos efektą akies dugno vaizduose šalina geriau už analogiškus metodus su afininiu, paprastu ir radialiniu modeliais.

Sukurtas skersinės chromatinės aberacijos šalinimo metodas pagrįstas kraujagyslių tinklo atpažinimu tikslumu prilygsta kalibravimo šablonais grindžiamiems skersinių chromatinių aberacijų šalinimo metodams.

Disertacijos struktūra

Disertaciją sudaro 4 skyriai ir literatūros sąrašas. Disertacijos skyriai: Įvadas, Kontūrų atpažinimo metodų tinkamumo kelio dangos kontūrams atpažinti tyrimas, Aberacijos ir vaizdų kokybė, Skersinės chromatinės aberacijos šalinimo metodas, Bendrosios išvados, Literatūra. Papildomai disertacijoje pateiktas iliustracijų, lentelių, simbolių ir žymėjimų sąrašas. Visa disertacijos apimtis 129 puslapiai, 58 numeruotos formulės, 54 paveikslėliai ir 8 lentelės. Disertacijoje remtasi 134 literatūros šaltiniais.

Bendrosios išvados

Pasiūlytas kelio dangos defektų kontūrų atpažinimo metodas kontūrą atpažįsta vidutiniškai 78% tikslumu lyginant su žmogaus apibrėžtu kontūru.

Disertacijoje pristatytas kelio dangos defektų kontūrų atpažinimo metodas grindžiamas prisitaikančiu binarizacijos slenksčiu leidžia pasiekti 25% didesnį tikslumą už aktyvaus kontūro metodą su prisitaikančiu binarizacijos slenksčiu.

Skersinės chromatinės aberacijos efektą šalinant akies dugno vaizduose su kalibravimo šablonais grindžiamais skersinių chromatinių aberacijų šalinimo metodais, tikslinga naudoti geriausius rezultatus užtikrinantį projekcinį modelį. Eksperimentiškai nustatyta, kad skersinės chromatinės aberacijos metodas grindžiamas projekciniu modeliu davė geriausių rezultatų ir RMSE paklaidą vidutiniškai sumažina 2,14 karto mėlynam kanalui ir 3,14 karto raudonam kanalui. Pakartojus bandymus po 20 kartų su skirtingomis atsitiktinėmis pradinėmis korekcijos koeficientų reikšmėmis abiem atvejais vidutinė dispersija mažesnė už 0,001. Blogiausių rezultatų davė radialiniai modeliai. Projekcinio modelio RMSE rezultatai yra $33-37$ % geresni už radialinio modelio su vienu parametru ir $13-18$ % geresni už radialinio su dviem parametrais. Nustatyta, kad projekcinis modelis tik nežymiai geresnis ($0-0{,}1$ %) už afininį ir ($0{,}48-3{,}83$ %) paprastą. Afininį arba paprastą modelius geriausiai naudoti kai reikalingas didesnis skaičiavimo greitis.

Skersinės chromatinės aberacijos šalinimo kokybei įvertinti panaudojus Suliejimo (M_{BM}), Chromatic Zipper (M_{ChZ}) ir Achromatic Zipper (M_{AChZ}) matus galima teigti, kad kalibravimo šablonais grindžiamas skersinės chromatinės aberacijos šalinimo metodas su projekciniu modeliu (KŠ) ir sukurtas skersinės chromatinės aberacijos šalinimo metodas grindžiamas kraujagyslių kontūrų tinklo atpažinimu (KA) leidžia reikšmingai sumažinti skersinės chromatinės aberacijos efektą, o skirtumas tarp abiejų metodų remiantis M_{ChZ} ir M_{AChZ} matais nėra reikšmingas. M_{BM} mato rodiklis parodė, kad su KŠ metodu vaizdo kokybė pagerėjo 13,1 %, o su KA – 6,8 %. Šis skirtumas remiantis Studento t-testu yra reikšmingas. M_{ChZ} mato rodiklis parodė, kad su KŠ metodu vaizdo kokybė pagerėjo 5,32 %, o su KA – 5,25 %. Ir M_{AChZ} mato rodiklis parodė, kad naudojant KŠ metodą vaizdo kokybė pagerėjo 2,45 %, o naudojant KA – 2,11 %. Kadangi, pagal du iš trijų matų skirtumas tarp metodų yra labai mažas, KA metodą galima naudoti vietoje KŠ, kai norima apsieiti be kalibravimo šabloninių vaizdų.

Vytautas Jakštys

KONTŪRO ATPAŽINIMO METODŲ TAIKYMAS AKIES DUGNO NUOTRAUKŲ KONTRASTIŠKUMO DIDINIMUI IR KELIO DANGOS DEFEKTŲ ATPAŽINIMUI

Daktaro disertacijos santrauka
Technologijos mokslai, informatikos inžinerija (07 T)
Redaktorė Jorūnė Rimeisytė

Vytautas Jakštys

APPLICATION OF CONTOUR DETECTION METHODS TO EYE FUNDUS IMAGE QUALITY ENHANCEMENT AND ROAD SURFACE DEFECT DETECTION

Summary of Doctoral Dissertation
Technological Sciences, Informatics Engineering (07 T)
Editor Janina Kazlauskaitė